

Design and development of radio frequency output window for circular electron-positron collider klystron

Zhijun Lu(陆志军), Shigeki Fukuda, Zusheng Zhou(周祖圣), Shilun Pei(裴士伦), Shengchang Wang(王盛昌), Ouzheng Xiao(肖欧正), UnNisa Zaib, Bowen Bai(白博文), Guoxi Pei(裴国玺), Dong Dong(董东), Ningchuang Zhou(周宁闯), Shaozhe Wang(王少哲), Yunlong Chi(池云龙)

Citation: Chin. Phys. B . 2018, 27(11): 118402. **doi:** 10.1088/1674-1056/27/11/118402
Journal homepage: http://cpb.iphy.ac.cn; http://iopscience.iop.org/cpb

What follows is a list of articles you may be interested in

Modeling and experimental studies of a side band power re-injection locked magnetron

Wen-Jun Ye(叶文军), Yi Zhang(张益), Ping Yuan(袁萍), Hua-Cheng Zhu(朱铧丞), Ka-Ma Huang(黄卡玛), Yang Yang(杨阳)
Chin. Phys. B . 2016, 25(12): 128402. **doi:** 10.1088/1674-1056/25/12/128402

A high-power subterahertz surface wave oscillator with separated overmoded slow wave structures

Guang-Qiang Wang(王光强), Jian-Guo Wang(王建国), Peng Zeng(曾鹏), Dong-Yang Wang(王东阳), Shuang Li(李爽)
Chin. Phys. B . 2016, 25(12): 128401. **doi:** 10.1088/1674-1056/25/12/128401

Theoretical investigation of frequency characteristics of free oscillation and injection-locked magnetrons

Song Yue(岳松), Dong-ping Gao(高冬平), Zhao-chuan Zhang(张兆传), Wei-long Wang(王韦龙)
Chin. Phys. B . 2016, 25(11): 118403. **doi:** 10.1088/1674-1056/25/11/118403

Mode analysis and design of 0.3-THz Clinotron

Shuang Li(李爽), Jian-Guo Wang(王建国), Guang-Qiang Wang(王光强), Peng Zeng(曾鹏), Dong-Yang Wang(王东阳)
Chin. Phys. B . 2016, 25(10): 108401. **doi:** 10.1088/1674-1056/25/10/108401

Power-combining based on master—slave injection-locking magnetron

Ping Yuan(袁萍), Yi Zhang(张益), Wenjun Ye(叶文军), Huacheng Zhu(朱铧丞), Kama Huang(黄卡玛), Yang Yang(杨阳)
Chin. Phys. B . 2016, 25(7): 078402. **doi:** 10.1088/1674-1056/25/7/078402

Design and development of radio frequency output window for circular electron–positron collider klystron*

Zhijun Lu(陆志军)[1,2,3,†], Shigeki Fukuda[1,4], Zusheng Zhou(周祖圣)[1,3], Shilun Pei(裴士伦)[1,3], Shengchang Wang(王盛昌)[1,3], Ouzheng Xiao(肖欧正)[1,3], UnNisa Zaib[1,3], Bowen Bai(白博文)[1,2,3], Guoxi Pei(裴国玺)[1,3], Dong Dong(董东)[1,3], Ningchuang Zhou(周宁闯)[1,3], Shaozhe Wang(王少哲)[5], and Yunlong Chi(池云龙)[1,3]

[1] *Institute of High Energy Physics, Chinese Academy of Sciences, Beijing* 100049, *China*
[2] *University of Chinese Academy of Sciences, Beijing* 100049, *China*
[3] *Key Laboratory of Particle Acceleration Physics and Technology, Institute of High Energy Physics, Chinese Academy of Sciences, Beijing* 100049, *China*
[4] *High Energy Accelerator Research Organization, KEK, Oho, Ibaraki* 305-0801, *Japan*
[5] *GLVAC Industrial Technology Research Institute of High Power Devices, Kunshan* 215300, *China*

(Received 25 July 2018; revised manuscript received 6 September 2018; published online 25 October 2018)

This paper presents the first phase of design, analysis, and simulation for the klystron coaxial radio frequency (RF) output window. This study is motivated by 800 kW continuous wave (CW), 650 MHz klystrons for the future plan of circular electron–positron collider (CEPC) project. The RF window which is used in the klystron output section has a function to separate the klystron from the inner vacuum side to the outside, and high RF power propagates through the window with small power dissipation. Therefore, the window is a key component for the high power klystron. However, it is vulnerable to the high thermal stress and multipacting, so this paper presents the window design and analysis for these problems. The microwave design has been performed by using the computer simulation technology (CST) microwave studio and the return loss of the window has been established to be less than −90 dB. The multipacting simulation of the window has been carried out using MultiPac and CST particles studio. Through the multipacting analysis, it is shown that with thin coating of TiN, the multipacting effect has been suppressed effectively on the ceramic surface. The thermal analysis is carried out using ANSYS code and the temperature of alumina ceramic is lower than 310 K with water cooling. The design result successfully meets the requirement of the CEPC 650 MHz klystron. The manufacturing and high power test plan are also described in this paper.

Keywords: klystron, coaxial radio frequency window, thermal stress, multipacting

PACS: 84.40.Fe, 29.20.Ej **DOI:** 10.1088/1674-1056/27/11/118402

1. Introduction

The Institute of High Energy Physics (IHEP), Chinese Academy of Sciences (CAS), has proposed a future plan of circular electron–positron collider (CEPC) in China,[1] which will be the biggest electron–positron collider in the world. Klystron is a critical component for an efficient and reliable operation of accelerator. As radio frequency (RF) power sources, 192 or even more high efficiency klystrons with a frequency of 650 MHz and a continuous wave (CW) output power of 800 kW are required. These klystrons are expected to be designed at IHEP and manufactured domestically in China. The specifications of CEPC klystron are listed in Table 1,[2] and we aim to obtain more than 65% efficiency for the first klystron and more than 80% for the future to reduce the cost of operation.

For the success of CEPC, the stable operation of klystrons is important, and the RF window used in the klystron is one of its key components. The RF output window is a critical part to transmit high RF power from klystron vacuum side to the external atmosphere with low power dissipation and no breakdown. For window design, it must have a capability of holding the klystron under pressure such as 10^{-7} Pa, and the good impedance matching is necessary. Furthermore, high power handling capability, excellent mechanical strength, uniform thermal distribution, and low probability of multipacting for ceramic window are required.

Table 1. CEPC klystron design parameters.

Frequency/MHz	650
Output power/kW	800
Beam voltage/kV	81.5
Beam current/A	15.1
Efficiency/%	> 80

Since it is the first time to design and manufacture such a high power klystron with a coaxial window at IHEP, a project team was formed to start the analysis and simulation. We made a strategy to manufacture a reusable klystron and RF window and proceeded one by one as shown in Fig. 1.[3]

*Project supported by Yifang Wang's Science Studio of the Ten Thousand Talents Project, China.
†Corresponding author. E-mail: luzj@ihep.ac.cn
© 2018 Chinese Physical Society and IOP Publishing Ltd

Now we changed to start from Fig. 1(b) to manufacture and test the klystron designed by classical approach. We have a plan to build the higher efficiency klystron in Fig. 1(c) adopting the recently developed bunching process improvements, such as core oscillation method (COM), bunch-align-compress (BAC), and core stabilization method (CSM).[4] Generally, the klystron is an amplifier of A to B class operation, but it is possible to have a higher efficiency by employing more cavities with 2nd and 3rd harmonics. Prior to building the tube, the manufacturing of the window itself must be performed and evaluated using the existing RF power source to ensure the power handling capability. Since the klystron has a response curve with power saturation, the window must be operated in a wide range of power from the linear region to the saturated power. The maximum rating of the window of 800 kW is at the saturated power.

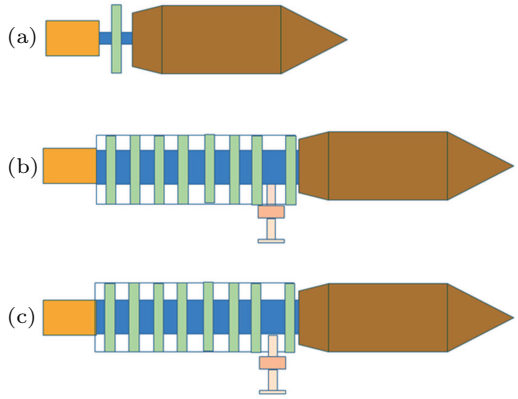


Fig. 1. (color online) Klystron development strategy: (a) beam test setup, (b) classical prototype, and (c) high efficiency prototype.

2. Window design

WR1500 (381 mm×190.5 mm) waveguide is used for transmitting the 650 MHz RF power from klystron to accelerator, but it is difficult to use the pillbox window with rectangular waveguide for the klystron output cavity because of its big size. The interference between the waveguide and the coil for the klystron is severe. The pillbox window has a difficulty in efficiently cooling the center of large aperture ceramic, and then the high temperature may result in a thermal stress that may cause ceramic failure.

Therefore, we use the coaxial structure coupling to the output cavity and then transfer the power to the WR1500 waveguide. There are three types of coaxial windows which are frequently employed in high power klystron, namely, (i) the cylindrical ceramic window coupling to the rectangular waveguide, (ii) the coaxial window with a choke structure in the inner and outer conductors, and (iii) the simple coaxial window having a hump structure. Type (i) shown in Fig. 2(a) has been used in many cases,[5] but the asymmetric position of transition in waveguide causes the nonuniform heating of the ceramic cylinder. Type (ii) shown in Fig. 2(b) is also frequently used to suppress the multipacting between the ceramic and inner or outer conductor.[6,7] Concerning the multipacting suppression for type (ii) window, a simulation was performed using Multipac 2.1[8] in a similar way as described in Section 4. In this case, it is effective to suppress the multipacting on the triple junction point at high power. While the electromagnetic field concentrates on the tip of the choke part which was very close to ceramic, it would cause multipacting due to a very high secondary emission coefficient of ceramic; the field may also lead to ceramic local overheating which was hard to cool down. Generally, the blazing of the choke structure window is very complicated if the window parts contain the hump structure to block the x-ray coming from the output cavity gap (Fig. 2(b)). Therefore, we choose the type (iii) window shown in Fig. 3.

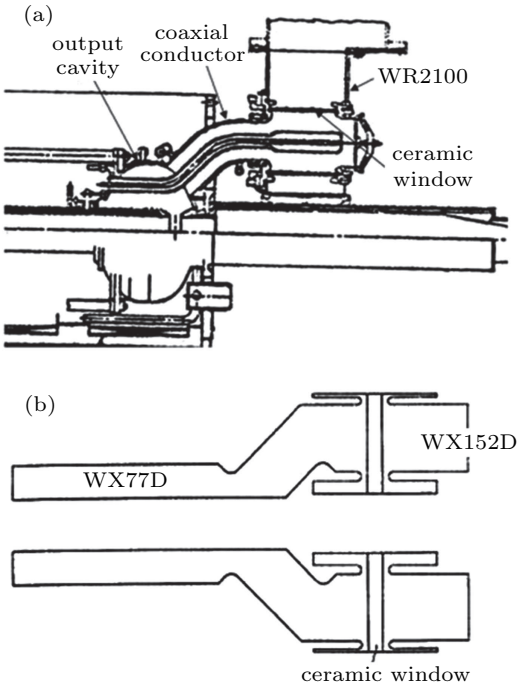


Fig. 2. (a) Type (i) window and (b) type (ii) window.

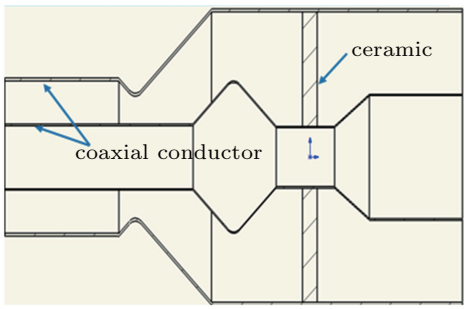


Fig. 3. (color online) Schematic of CEPC klystron RF output window (type (iii)).

A schematic of the CEPC 650 MHz klystron window is shown in Fig. 3, in which two humps are included on the coax-

ial conductors. These humps are designed to protect the ceramic surface from electrons/x-ray bombardment generated at the output cavity gap, which may be harmful to the ceramic window. The radius of the inner conductor of window is chosen to be slightly smaller than the inner radius of the coaxial conductor to the output cavity to obtain the impedance matching at the frequency of 650 MHz. Using computer simulation technology (CST) microwave studio,[9] type (iii) window is designed. The ceramic thickness is about 11 mm. With high purity alumina (99.5%), we obtain good results for the dielectric loss in the ceramic and mechanical strength to thermal stress and atmosphere pressure.

To have a good impedance matching, the geometrical design of the window is performed by CST microwave studio code. From the operational requirement, the voltage standing wave ratio (VSWR) of the window is lower than 1.05, and it corresponds to S_{11} lower than -32.3 dB. After the optimization of the geometrical parameters, we obtain -90 dB for S_{11} at the operation frequency and less than -30 dB at ± 50 MHz bandwidth as shown in Fig. 4. So the S-parameter in our design satisfies the requirement.

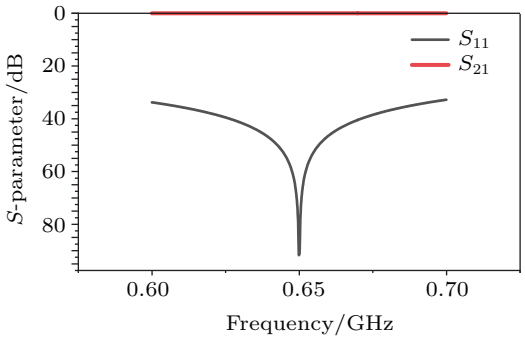


Fig. 4. (color online) The return loss S_{11} and insert loss S_{21}.

In order to investigate the mechanical tolerance, we investigate the dimension variation from the optimum value and evaluate the S-parameter and bandwidths. The parameter sensitivity analysis shows that for a ± 0.3 mm change in diameter for most of the window components, S_{11} is changed from -90 dB to -60 dB at 650 MHz, and less than -30 dB at ± 50 MHz bandwidth is also obtained. This is achievable and not difficult. The most sensitive parameter is the ceramic thickness, and S_{11} is changed from -90 dB to -45 dB at 650 MHz for a ± 0.2 mm variation. Concerning the ceramic, a purity of 99.5% gives the dielectric constant ε of 10 at the frequency of 650 MHz (provided by Toshiba), and this is used in the simulation. In the high power operation, it is possible that the ceramic temperature goes high, which changes ε from 10 to 9.9, resulting in the small change of the performance.

3. Thermal analysis

Besides the usual microwave design of the window, we should pay attention to the window cooling for two reasons. The first reason is that cooling the coaxial coupler or window is not easy, especially for the coaxial inner conductor. The second reason is that a high temperature rise is caused by thermal loss in the inner coaxial line and dielectric loss of the alumina ceramic during the high power operation, which may result in a high thermal stress in ceramic or possibly breaking of the ceramic window. Multipacting on the ceramic surface is another possible source of temperature rise. In this section, the window cooling is analyzed.

Water cooling mechanism is preferred to be considered because of its powerful cooling capability. In CEPC klystron, the power rating of CW klystron reaches 800 kW, and the thermal loss of the window is estimated to be about 800 W. Most of the loss concentrates on the inner conductor, and the heat transferred to the ceramic results in several hundred degrees Celsius. Therefore, only forced air cooling might not be sufficient.

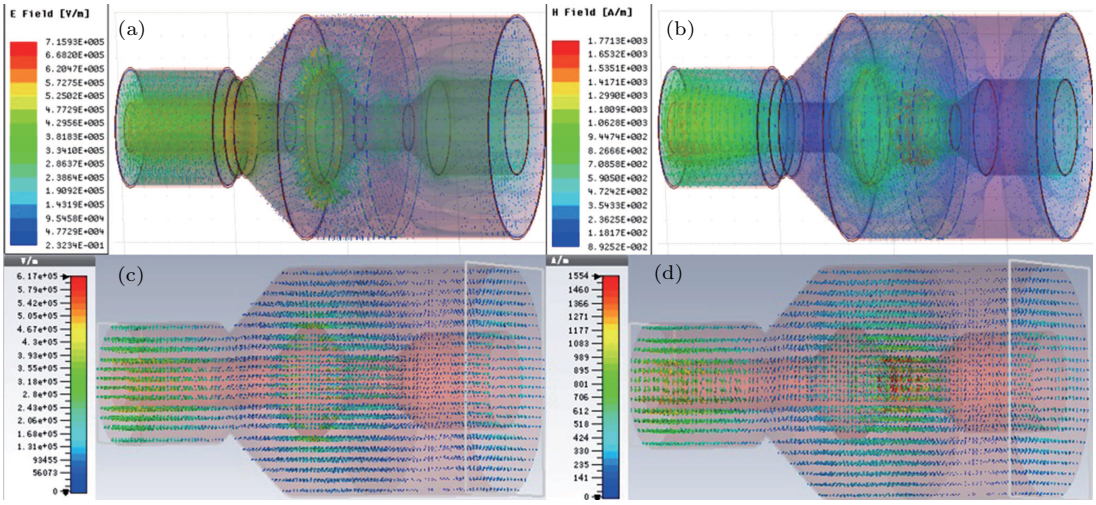


Fig. 5. (color online) Electromagnetic field simulation by ANSYS and CST. (a) and (b) are for electric field and magnetic field calculated by ANSYS, while (c) and (d) are for electric field and magnetic field calculated by CST, respectively.

Figure 5 shows the electromagnetic field (E-field) calculated by ANSYS[10] and CST codes. The results for electromagnetic field simulation are almost the same in both codes. The maximum of E-field is around 6×10^5 V/m, and the maximum of H-field is about 1600 A/m. The E-field in this type of RF window shows no concentration on the ceramic surface. It is simulated that the most of the loss occurs on the inner conductor, so special consideration should be given to cooling it. Because it is difficult to make a water channel from the output cavity of the klystron, cooling of the inner conductor around the window is introduced from the transition side of the waveguide (air side). In order to obtain better cooling, double piping structure is adopted after negotiating with Toshiba electron-tube division (TETD), and hence good cooling for the humps and inner conductor is achieved. The outer conductor of the ceramic window is also water-cooled.

The thermal simulation in CST code and ANSYS code is carried out by setting the convective heat transfer coefficient and radiation coefficient. But since the radiation effect is very small in our temperature range, it is sufficient to consider the thermal convection.[11]

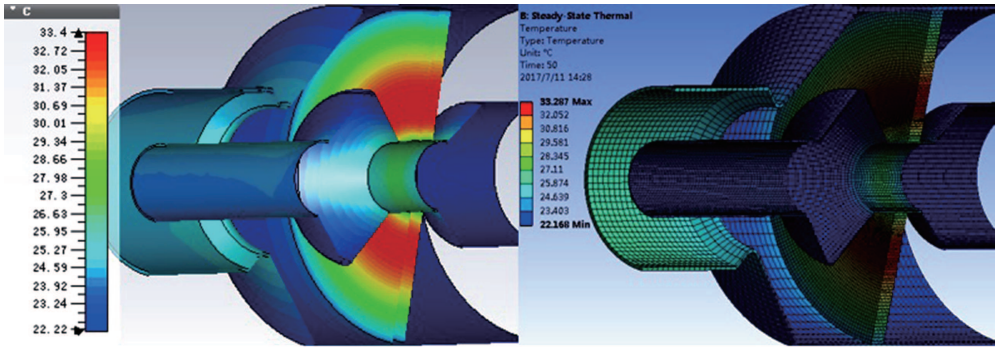
The Reynolds number Re is given by

$$Re=\frac{du\rho}{\lambda}, \tag{1}$$

where d is the diameter of the cooling water channel, u is the velocity of water which is chosen to be 0.4 m/s, ρ is the density of water, and λ is the thermal conductivity. We assume that the input water temperature is 22 °C. The heat transfer coefficient α is calculated by

$$\alpha=0.023f\frac{\lambda}{d}Re^{0.8}Pr^n, \tag{2}$$

where f is the fixed coefficient of the special condition, Prandtl number $Pr=6.22$ corresponds to the input water temperature, and $n=4$ is chosen because water is heated. The results of heat transfer coefficient and thermal loss in copper and alumina ceramic are used in CST and ANSYS.



(a) (b)

Fig. 6. (color online) Thermal simulation in (a) CST and (b) ANSYS.

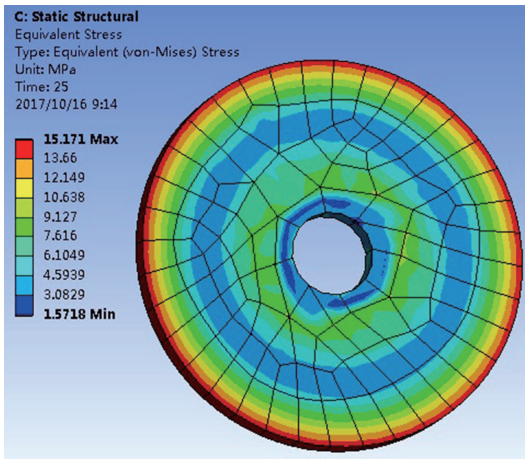


Fig. 7. (color online) Thermal stress on the ceramic surface.

The thermal simulation results in both codes agree well. Figure 6 shows the simulation results when the water cooling is supplied in the inner and outer conductors. The difference between the maximum and minimum temperatures in ceramic plate is about 8 °C, and the maximum thermal stress caused by the temperature difference is about 15 MPa, as shown in Fig. 7. This is much smaller than the alumina ceramic stress capacity of 320 MPa. And the structure deformation by the temperature difference is in a micron level. Since the thermal conductivity of copper is high to transfer the heat from the conductor to the cooling water, the cooling of the entire window is sufficient even in the case of the maximum temperature on the surface of ceramic which is about 33 °C. So far, in this analysis, we have not considered the window failure due to the thermal runaway by the abnormal phenomena of local heating. It should be the next topic.

4. Multipacting analysis

The destruction of klystron output ceramic windows is frequently caused by multipacting or surface discharge.[12] Multipacting directly results in surface local overheating of alumina ceramic and ceramic cracking or pinhole, leading to

the vacuum leak of the tube. Ceramic window breakdown is one of the most frequent causes of the klystron failure. In this section, multipacting phenomenon is studied and described.

Multipacting is a common phenomenon in the ceramic window and in some cases it causes serious damages. Multipacting is induced by the electrons emitted from the metal surface and the triple junction around the ceramic brazing area. The emitted electrons may collide with the ceramic surface interacting with the RF field, and as a result more electrons are emitted if the secondary electron emission yield (SEY) on the ceramic is high. If this process is repeated, local heating due to this electron multipacting bombardment leads to breakdown. Therefore, avoiding serious multipacting is achieved not only by designing the structure but also by choosing a low SEY ceramic surface.

The ceramic coating with thin coating of TiN (low SEY characteristic) is a popular way to suppress secondary emission. The maximum SEY value can be as high as 5.8 for such high purity alumina ceramic if there is no coating on the ceramic surface. Since TiN is a resistive material and a thick film increases loss, there is an optimum thickness to effectively suppress the secondary electrons. TiN coating thickness is chosen to be about 5 nm from the past experience as described in Ref. [13]. In the case of 5 nm coating, the resistivity of TiN film is very small, so there is little effect on the S-parameter as shown in Fig. 4 after coating with TiN. And, many high power klystrons also employ TiN coating on the ceramic. Therefore, this process is simulated to confirm the TiN coating effect. The SEY curves of ceramic with and without coating are shown in Fig. 8. Since multipacting is a particular phenomenon in vacuum, TiN is only coated on the vacuum side, but coating is required in the whole area from the inner diameter to the outer diameter.

From Fig. 8, we may deduce that multipacting possibly occurs over a wide range of electron impact energy from 100 eV to 10000 eV in the case without coating, while SEY substantially decreases and the multipacting range possibly becomes narrower in the case with TiN coating.

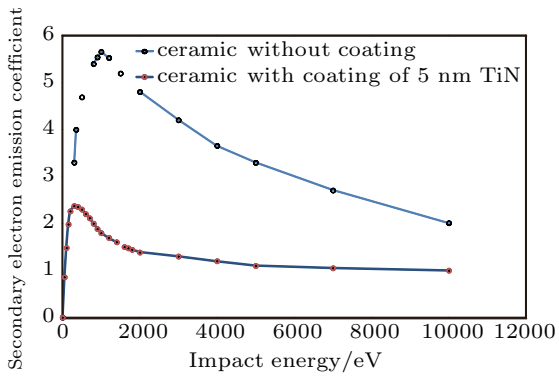


Fig. 8. (color online) Secondary electron emission coefficient of 99.5% alumina ceramic without and with 5 nm TiN coating.

The multipacting simulation is performed using the code MultiPac as shown in Fig. 9. In this code, initial electron source is automatically surveyed along our set boundary of the window, where c_0 is the initial free electron number in the volume, c_{20} is the free electron number after 20 impacts, Ef_{20} is the average impact energy of the last impact in eV, and e_{20} is the secondary electron number after 20 impacts. Some simulation results are shown in Fig. 9 in the cases of with and without TiN coating. In this figure, the horizontal axis shows the average incident power in kW, and the power up to 800 kW is the only important part due to our output power specification. If Ef_{20} is in the high SEY range, the multipacting may be severe.

In the case without coating, e_{20}/c_0 increases sharply at power levels around 300 kW, 600 kW, and 800 kW as shown at the bottom of Fig. 9(a). At these power levels, most of the impact energy of electrons ranges from 100 eV to several thousands of eV, which is in the high SEY range. Since the secondary electron number reaches 10^5 times of the initial number of electron in average, multipacting may occur severely. The electron trajectory due to multipacting is shown in Fig. 10.

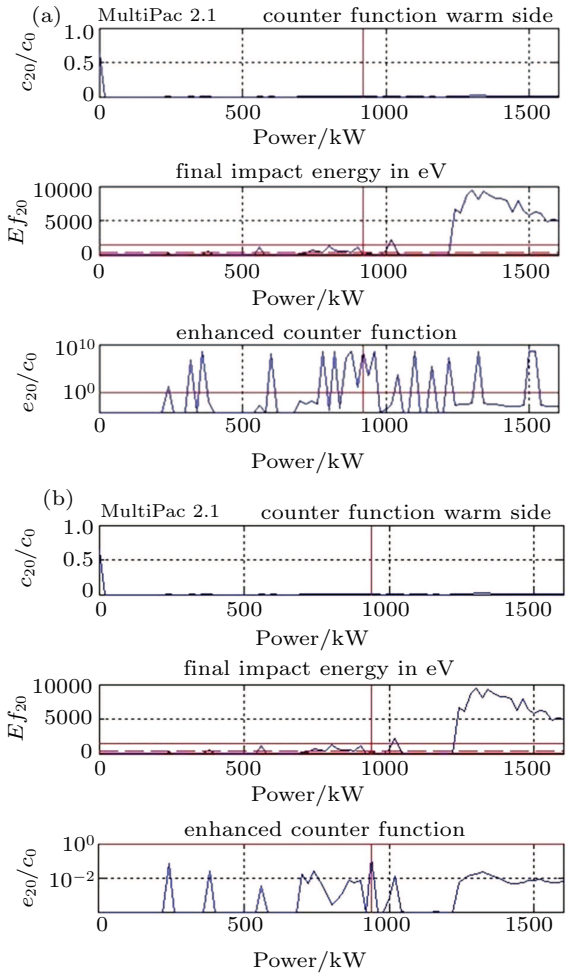


Fig. 9. (color online) Multipacting result in MultiPac version 2.1. (a) Ceramic without coating, and (b) ceramic with 5 nm TiN coating.

In the case of 5 nm TiN coating in Fig. 9(b), though the impact energy is also between 100 eV and 1000 eV where

SEY is larger than 2, the secondary electron number is quite low and it is difficult for multipacting or electron avalanche to continue. This simulation result of a significant reduction in the secondary electron number with the TiN coating is in good agreement with CST in Fig. 11, which shows the numbers of secondary electrons on ceramic surface with and without the coating at 800 kW operating power.

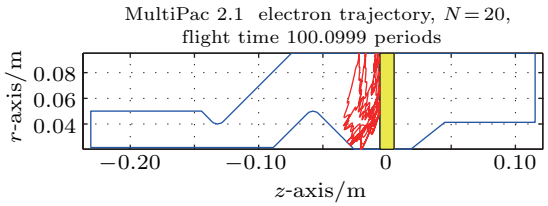


Fig. 10. (color online) Electron trajectory of multipacting in MultiPac.

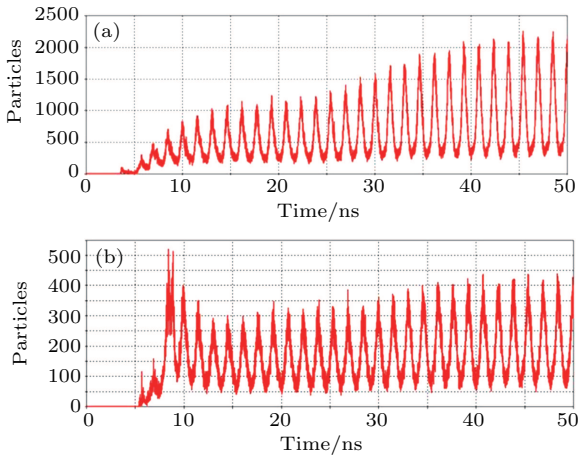


Fig. 11. (color online) Secondary electron emission on the ceramic (a) without and (b) with 5 nm TiN coating in CST.

From this result, it is concluded that multipacting may occur without coating, but it is suppressed dramatically with coating.

5. Hot test plan

Since this window is used in the klystron, one side of the window is evacuated. Therefore, two windows connected by the waveguide structure in vacuum are required to be evaluated for their performance similar with the klystron window. The doorknob coupler is designed to achieve water cooling for inner conductor. The pressure inside should be as low as that of klystron, which is about 10^{-7} Pa. The windows and coupler will be baked before testing.

The hot test includes high power capability of the ceramic window, requiring a proper cooling system with inlet and outlet of water supplied from the doorknob side through double piping structure.

We will increase the power step by step as in the klystron high power operation test. In this test, a solid state amplifier (SSA) with 150 kW CW is available at IHEP. The power transmission test with load is planned followed by the full reflection test by changing the phase. By this test, we can equivalently evaluate the power capability of 600 kW.

The ceramic coating is important; therefore, these windows manufactured by TETD will be coated with 5 nm TiN(O) film on the ceramic surface. The viewport and arc-detector are used to detect multipacting or arcing problems.

6. Conclusion

We have finished the simulation of the RF coaxial output window to be used in the CEPC 650 MHz, 800 kW CW klystron. We have compared several types of windows and chosen the type (iii) window. The RF design has been fulfilled and the *S*-parameter has been optimized. The thermal loss and multipacting in ceramic have also been considered in the high power operation. Good window cooling has been successfully introduced after the thermal analysis. After the simulation using CST and MultiPac, it is successfully shown that the suppression of the multipacting with 5 nm TiN coating has been achieved. We have finished the mechanical design and started to manufacture it. The high power test scheme is also described.

Acknowledgement

The author wants to thank the mechanical design group member Mr. Wang Jianli for his work and suggestions.

References

[1] *Preliminary Conceptual Design Report* IHEPAC 201501
[2] Zhou Z S, Fukuda S, Wang S C, Xiao O Z, Dong D, Zaib U N, Lu Z J and Pei G X 2016 *The 7th International Particle Accelerator Conference* May 8–13 2016 Busan, Korea, p. 3891
[3] Zaib U N, Fukuda S, Zhou Z S, Wang S C, Xiao O Z, Dong D, Lu Z J and Pei G X 2017 *Chin. Phys. Lett.* **34** 012902
[4] Hill V C R, Burt G, Constable D, Lingwood C, Marrelli C and Syratchev I 2017 *2017 Eighteenth International Vacuum Electronics Conference (IVEC)*, April 24–26, 2017 London, UK
[5] Konrad G T 1977 *IEEE Trans. Nucl. Sci.* **24** 1689
[6] Naito F, Sakai H, Yoshimoto S, Mizuno H, Akasaka N, Kageyama T, Takeuchi Y, Akai K, Ezura E, Nakanishi H and Yamazaki Y 1998 *The Input Coupler For KEKB ARES Cavity* KEK Preprint 98–44
[7] Isagawa S, Takeuchi Y, Baba H, Tanaka J, Ohya K, Kawakami Y and Hosoi S 1987 *Proceedings of the 12th IEEE Particle Accelerator Conference* March 16–19, 1987 Washington DC, USA, p. 1934
[8] Ylä-Oijala P, Lukkarinen J, Järvenpää S, Ukkola M 2001 *MultiPac 2.1 Multipacting Simulation Toolbox with 2D FEM Field Solver and MATLAB Graphical User Interface*, User's manual, Rolf Nevanlinna Institute, Helsinki
[9] http://www.cst.com
[10] http://www.ansys.com/Products/Platform
[11] Yang S M 2010 *Heat Transfer* (Beijing: Higher Education Press) (in Chinese)
[12] Saito Y 1995 *IEEE Trans. Dielectr. Electr. Insul.* **2** 243
[13] Saito Y 1989 *Rev. Sci. Instrum.* **60** 1736